Effects of Slit3 silencing on the invasive ability of lung carcinoma A549 cells

CHAO ZHANG[1,2*], HUI GUO[1*], BIN LI[1], CHENGZHI SUI[3], YUAN ZHANG[1], XIANYUAN XIA[1], YING QIN[1], LIYING YE[1], FU'AN XIE[1], HENG WANG[1], MINGJING YUAN[1], LI YUAN[1] and JUN YE[1]

[1]State Key Laboratory of Cellular Stress Biology, School of Life Sciences, Xiamen University, Xiamen, Fujian; [2]Geneseeq Technology Inc., Nanjing, Jiangsu; [3]The First Affiliated Hospital of Xiamen University, Xiamen, Fujian, P.R. China

Received April 9, 2015; Accepted May 18, 2015

DOI: 10.3892/or.2015.4031

Abstract. Slit proteins function as chemorepellents in axon guidance and neuronal migration by binding to cognate Robo receptors. The Slit/Robo signaling pathway is also involved in the regulation of tumor cell metastasis. However, whether the Slit/Robo signaling pathway exerts prometastatic or antimetastasis functions remains controversial. To date, most of the research on Slit/Robo has focused on Slit2, and the effects of Slit3 on metastasis remain largely unknown. Based on the Oncomine database, overall expression of *Slit3* is low in tumor tissues compared to its level in normal tissues. The underlying mechanism for slit3 silencing in tumor tissues is likely related to hypermethylation of the slit3 promoter. However, lung carcinomas appear to be an exception. Several studies have reported that the frequency of *Slit3* methylation in lung cancers is far lower than the frequency of *Slit2*. In the present study, high *Slit3* expression at the mRNA level, yet not at the protein level, was detected in lung adenocarcinoma A549 cells. The function of Slit3 in tumor migration and invasion was examined by silencing of *Slit3* expression in A549 cells. Silencing of *Slit3* promoted proliferation, migration and invasion of A549 cells and induced epithelial-mesenchymal transition by downregulation of E-cadherin and upregulation of vimentin. The inhibitory effects of Slit3 on tumor migration and invasion are likely related to matrix metalloproteinases (MMPs). Silencing of *Slit3* in the A549 cells enhanced MMP2 and MMP9 expression. These results indicate that Slit3 is a potential tumor suppressor in lung adenocarcinoma.

Correspondence to: Professor Jun Ye or Professor Li Yuan, State Key Laboratory of Cellular Stress Biology, School of Life Sciences, Xiamen University, Xiamen, Fujian, P.R. China
E-mail: jye@xmu.edu.cn
E-mail: yuanli@xmu.edu.cn

*Contributed equally

Key words: Slit3, lung carcinoma, A549, migration, invasion, MMP2, MMP9, epithelial-mesenchymal transition

Introduction

Slits are large secreted proteins (up to 200 kDa) that regulate neuronal orientation and branching during nervous system development by signaling through cognate Robo receptors that consist of four known members (Robo1-4). In mammals, three *Slit* genes, *Slit1*, *Slit2* and *Slit3*, have been identified. All the Slit proteins contain four leucine-rich repeat domains, six EGF domains, a laminin G domain and a cysteine-rich domain (1). All three Slit proteins are proteolytically cleaved into a large N-terminal fragment (140 kDa) and a shorter C-terminal fragment (50-60 kDa) (2,3). The majority of the N-terminal fragment and full-length Slits are membrane-associated, which mediates their function. The C-terminal fragment is more diffuse and although its function remains largely unknown, Condac *et al* recently reported the pro-coagulation effects of the Slit3 C-terminal fragment by neutralizing the anticoagulant activity of heparin (4).

Slit1 expression is specific to neurons, while *Slit2* and *Slit3* are detected in various tissues, such as the lung, kidney and heart (5,6). Compared with normal tissues, *Slit* genes are epigenetically silenced in a wide variety of cancers, indicating that Slits are potent tumor suppressors (7,8). To date, most studies involving the effects of Slits on tumors have focused on Slit2, including epigenetic modifications (9,10), expression in various types of cancer and inhibition of tumor growth, metastasis (11-17) and angiogenesis (18,19). Although most results support the inhibitory effects of Slit2 on tumor growth and metastasis, the role of Slit2 in growth and metastasis is still controversial. Several studies have validated a stimulative role of Slit2 on tumor growth and metastasis (20-22), and this discrepancy reflects the complexity of Slit/Robo signaling in different types of cancers.

Slit3 shares a high level of homology with Slit2, both with the same proteolytic cleavage site, *TSPCD*, at the beginning of the 6th EGF repeat (2). *Slit3* is detected in various normal tissues, with skin, brain cerebellum and lung having the highest expression levels (8). Genetic inactivation of *Slit3* in mice revealed multiple roles of *Slit3* in organ development, particularly in the diaphragm and kidney (23,24). In the vascular system, Slit3 is secreted by endothelial cells and vascular smooth muscle cells to stimulate angiogenesis by binding to the Robo4 receptor (25,26). Similar to Slit2,

frequent hypermethylation of promoters is the main cause of *Slit3* gene silencing in most cancers (8,27,28). Lung carcinomas appear to be an exception. The frequency of *Slit3* methylation in lung cancers is far less than *Slit2* (8,29), indicating that an alternative mechanism apart from methylation is responsible for the downregulation of *Slit3*. Recombinant Slit3 was reported to inhibit the migration of melanoma cells (30); the second leucine-rich repeat domain is sufficient to induce such repressive effects (31). Reduction of miR-218, which resides in the introns of the *Slit2* and *Slit3* genes, causes downregulation of *Slit3*, resulting in promotion of metastasis in thyroid cancer (32). *Slit3* overexpression in human breast carcinoma cells resulted in tumor growth by suppressing *CXCR4* expression (17). These results suggest the negative regulation of Slit3 on tumor growth and metastasis, similar to the most reported functions of Slit2. However, the functions of Slit3 in lung carcinoma have not been widely reported.

In the present study, we investigated the effects of Slit3 on lung carcinoma cells by *Slit3* gene silencing in A549 cells, which have a high level of *Slit3* expression compared to other cancer cell lines. We validated the inhibitory effects of Slit3 on proliferation, migration and invasion in the cells, confirming a potential tumor-suppressor role of slit3 in lung carcinoma.

Materials and methods

Cell culture. Human glioblastoma U87MG cells, and human normal lung fibroblasts (HFL-1) were purchased from the National Platform of Experimental Cell Resources for Sci-Tech (Beijing, China). Human lung adenocarcinoma A549, Spc-a-1 and Ltep-a-2 cells were purchased from the Cell Resource Center at the Institute of Life Sciences, Chinese Academy of Science (Shanghai, China). All cells were cultured in high-glucose Dulbecco's modified Eagle's medium (DMEM; HyClone, Logan, UT, USA) supplemented with 10% fetal bovine serum (FBS; Gibco-BRL, Carlsbad, CA, USA).

Lentiviral infection. shRNA *Slit3* oligos were annealed and cloned into the lentiviral vector pLentiLox 3.7 (a gift from Professor Jiahuai Han, State Key Laboratory of Cellular Stress Biology, School of Life Sciences, Xiamen University, China). The *Slit3* N-terminal (33aa-1120aa, ~140 kDa) was amplified from pSecTag2B-hSlit3 (gift from the Institut National de la Santé et de la Recherche Médicale, Paris, France) and subcloned into the lentiviral expression vector pBobi (gift from Professor Jiahuai Han) with a myc tag at the carboxyl terminus, and the same vector encoding GFP was used as a control. Virus stocks were prepared by co-transfecting pll3.7 or pBobi with two packaging plasmids (pHR and pVSVG) into 293T cells. Viral supernatants were harvested after 48 h, filtered and centrifuged (90 min at 75,000 x g). A549 cells were infected with pll3.7-*Slit3*-shRNA in the presence of 8 μg/ml Polybrene (Sigma, St. Louis, MO, USA) for two days. Infected A549 cells were sorted by clone picking.

Real-time quantitative PCR. Total RNA was extracted with TRIzol reagent (Life Technologies, Carlsbad, CA, USA). cDNA for the PCR template was generated using the ReverTra Ace qPCR RT kit (FSQ-101; Toyobo, Osaka, Japan) as recommended by the manufacturer's protocols. Primer sequences are listed in Table I. Real-time PCR was performed in an MJ Mini System (Bio-Rad) using Thunderbird SYBR qPCR Mix (QPS-201; Toyobo). Amplification was performed under the following conditions: 95˚C for 1 min followed by 40 cycles at 95˚C for 15 sec, and 62˚C for 45 sec. To normalize the real-time PCR results, *GAPDH* was used as an internal control. Relative genes expression in various tumor cell lines was calculated using the Livak and Schmittgen (33) method and compared with the U87MG cells.

Table I. Primers for real-time quantitative PCR.

hSLIT1-F	GCAATTCCACACCGTTGAGC
hSLIT1-R	AGCTGAGTTGACATCCACGG
hSLIT2-F	TGAAGGTCTTGCCGAAAGGTAT
hSLIT2-R	AAAGCGTGCTTATTCTGTTGTT
hSLIT3-F	GCGATTTGGAGATCCTTACCCT
hSLIT3-R	GCAGTACAGGTGGTTGGAGTGG
hROBO1-F	GCATCGCTGGAAGTAGCCATACT
hROBO1-R	CATGAAATGGTGGGCTCAGGAT
hROBO2-F	GGGTTACTACATCTGCCAGGCTT
hROBO2-R	AGGTGGAGGTCTATCTGTCAAAACAT
hROBO3-F	CAGTGTCCGATGGAAGAAGG
hROBO3-R	GTCCATCTCCTGCACATTGG
hROBO4-F	GACACTTGGCGTTCCACCTC
hROBO4-R	AGAGCAAGGAGCGACGACAG
hMMP2-F	CTTCTTCCCTCGCAAGCC
hMMP2-R	ATGGATTCGAGAAAACCG
hMMP9-F	ACGCAGACATCGTCATCC
hMMP9-R	CCACAACTCGTCATCGTC
hGAPDH-F	GGCTGAGAACGGGAAGCTTGTCAT
hGAPDH-R	CAGCCTTCTCCATGGTGGTGAAGA

Immunofluorescence. Cells were fixed with 4% paraformaldehyde/phosphate-buffered saline (PBS) for 15 min at room temperature. Fixed cells were washed twice with PBS and permeabilized with 0.25% Triton X-100/PBS for 15 min. Cells were blocked with 1.0% FBS/PBS for 1 h and labeled with rabbit polyclonal primary antibody for tubulin (T3526; Sigma) at a 1:80 dilution in 0.1% BSA/PBS buffer with 0.05% Tween-20 (PBST) at 37˚C for 1 h. After incubation, the cells were washed 3 times with PBST and incubated with Alexa Fluor 594-conjugated goat anti-rabbit secondary antibody (A11037; Invitrogen) at a 1:1,000 dilution at room temperature for 1 h in the dark. After washing with PBST, the cells were stained with 4',6-diamidino-2-phenylindole (DAPI) for 5 min. After extensive washing, the cells were examined and recorded with an inverted fluorescence microscope (IX71; Olympus, Japan) equipped with a SPOT Insight QE CCD camera.

Cell proliferation assay. A total of 500 cells were seeded/well in 96-well microplates (Sunub, Shanghai, China) and cultured for 4 consecutive days. The medium was changed every other day. On each day, one group of culture media was replaced with 100 μl serum-free fresh medium containing 10% MTT

(Sigma) and maintained at 37˚C for 4 h. After discarding the medium, 150 μl of dimethylsulfoxide (DMSO) was added to each well to dissolve MTT formazan. Optical densities were measured at 560 nm with a microplate reader (Multiskan MK3; Thermo Fisher Scientific, USA).

Cell migration and invasion assays. Cell migration was assessed by a wound healing recovery assay. Cells that were 90% confluent in a 24-well plate (Sunub) were scratched with a 200-μl pipette tip to form wound gaps. After washing out cell debris, the wound gaps were photographed under a microscope at a magnification of x40 to acquire a baseline image. The cells were then cultured in DMEM for the indicated time periods and photographed to obtain the second set of images. Gap width was measured using Image-Pro Plus 6.0 software. Cell migration was quantitatively analyzed by subtracting the gap width of the second image from the baseline image.

Cell invasion was assessed by the Matrigel invasion assay. Chambers (8 μm; Millipore, Billerica, MA, USA) were coated with 20 μl diluted Matrigel (0.1 mg protein/ml; BD) for 30 min at 37˚C and inserted into a 24-well plate. A total of $1x10^4$ cells/chamber in 100 μl serum-free DMEM were plated on the upper Matrigel-coated chambers. Medium in the lower chambers contained 10% FBS as the source of chemoattractant. The plates were incubated for 24 h at 37˚C. Cells that had invaded the lower surface at 37˚C were fixed with methanol and stained with crystal violet. Three random fields were counted under a light microscope.

Gelatin zymography. A total of 2 million cells were cultured in a 6-cm dish (Sunub) with 5 ml DMEM (10% FBS) for 8 h. Media were replaced with 2 ml serum-free DMEM and incubated for an additional 12 h. The conditioned media was collected and filtered with a 0.22-μm filter (Millipore). A total of 10 μl of conditioned media was mixed with 10 μl sample buffer [0.25 M Tris-HCl, pH 6.0, 8.5% glycerol, 4% sodium dodecyl sulfate (SDS) and 0.01% bromophenol blue] and electrophoresed on a 7.5% SDS-polyacrylamide gel containing 2 mg/ml gelatin (Sigma). After electrophoresis, the gel was washed 3 times for 10 min in 2.5% Triton X-100 and placed in incubation buffer (50 mM Tris-HCl, pH 7.6, 10 mM $CaCl_2$, 50 mM NaCl and 0.05% Brij-35) overnight at 37˚C. After incubation, the gel was stained with a solution of 0.25% Coomassie blue R250, 40% methanol and 10% acetic acid for 1 h at room temperature and destained with 40% methanol and 10% acetic acid until the protein bands were apparent.

Immunoblotting. To detect E-cadherin and vimentin, the cells were washed with cold PBS (pH 7.4), incubated with cold RIPA lysis buffer (P0013; Beyotime, China) on ice for 10 min, and collected with a scraper. Lysates were then centrifuged at 12,000 x g for 10 min. To detect membrane-associated Slit3 protein, a Qproteome Cell Compartment kit (Qiagen, Hilden, Germany) was used to isolate the protein. Protein samples were boiled at a ratio of 3:1 with sample buffer (250 mM Tris-HCl, pH 6.8, 40% glycerol, 20% mercaptoethanol, 8% SDS and 0.04% bromophenol blue) and separated by SDS-PAGE. Following electrophoresis, proteins on the gel were transferred to an Immobilon-P membrane (PVDF; 0.45 μm; Merck Millipore, Molsheim, France), which was blocked with 5% skim milk powder dissolved in TBS buffer with 0.05% Tween-20 (TBST). After washing, the membranes were incubated with rabbit polyclonal primary antibody for Slit3 (AB5703P; Merck Millipore) at a 1:500 dilution, rabbit monoclonal primary antibody for E-cadherin (#3195; Cell Signaling) at a 1:1,000 dilution, rabbit polyclonal primary antibody for vimentin (sc-5565; Santa Cruz) at a 1:1,000 dilution, mouse monoclonal antibody for α-tubulin (T6074; Sigma) at a 1:4,000 dilution and appropriate horseradish peroxidase-linked secondary antibodies at a 1:2,000 dilution. After washing 3 times with TBST, the bound antibody was developed using the ECL Plus Western Blotting Detection System (Thermo, USA).

Statistical analysis. GraphPad Prism software was used for all statistical analysis. Quantitative data are expressed as the mean ± SD and were compared using the unpaired Student's t-test.

Results

Slit and Robo expression in the lung carcinoma cell lines. The Oncomine database indicates that *Slit3* expression is downregulated in lung carcinoma compared to normal tissues (34,35). To verify the results in the tumor cell lines, we examined Slit and Robo expression in three lung adenocarcinoma cell lines (A549, Spc-a-1 and Ltep-a-2). Since *Slit3* has been reported to be overexpressed in gliomas and is considered a biomarker for gliomas (36), we used the glioblastoma cell line U87MG as a positive control for *Slit3*.

Slit1 expression was not detected in any of the cell lines analyzed. *Slit2* was detected in all of the cell lines and in general maintained a relatively lower expression when compared with that in the U87MG cells (Fig. 1A). *Slit3* was only detected in the A549 and U87MG cells. A549 cells showed high *Slit3* expression levels that were nearly 9-fold more than that of the U87MG cells. Of the three lung adenocarcinoma cell lines, high *Slit3* expression was only detected in the A549 cells, indicating cell-specific *Slit3* expression. However, high *Slit3* expression in the A549 cells was not evident at the protein level. Although Slit3 is a secreted protein, both ELISA of the cell supernatant and immunoblotting of the cell lysates (up to 80 μg of total loading protein) did not detect Slit3 (data not shown). We theorized that the membrane-associated characteristics of Slit and the relatively low amount of Slit3 may account for the lack of Slit3 detection in the supernatant and cell lysates. Unexpectedly, immunofluorescence only detected a very weak signal on the A549 cell surface (data not shown).

Robo receptors are heterogeneously expressed by tumor cell lines. While Robo2 was not detected in any of the cell lines assayed, Robo1 was detected in all of the cell lines. A549 cells maintained a relatively high level of Robo1 expression compared with the other cell lines. Robo3 and Robo4 were only detected in the U87MG and A549 cells, yet not in the Spc-a-1 and Ltep-a-2 cells (Fig. 1B).

Slit3 knockdown in A549 cells. To evaluate the role of Slit3, A549 cells were transduced with the VSVG pseudotyped lentivirus plasmid (pLL3.7) for stable *Slit3* silencing (A549-shRNA) or an empty control plasmid without *Slit3*-shRNA insertion

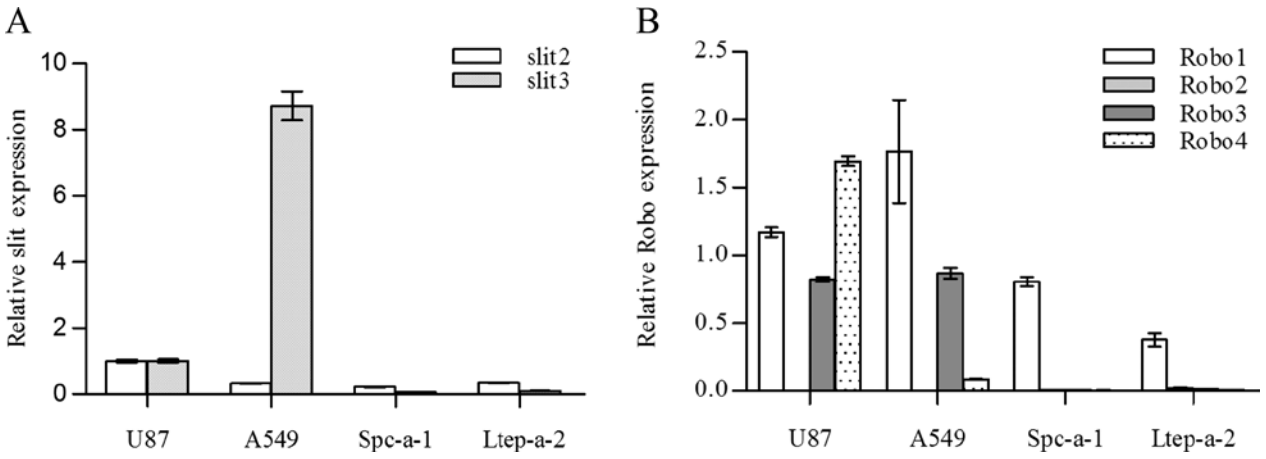

Figure 1. Analysis of *Slit* and *Robo* expression in tumor cell lines. (A) *Slit2* and *Slit3* were examined by real-time quantitative PCR. Data were first normalized to *GAPDH* and then normalized to the values of U87MG cells. Each sample was analyzed in triplicate and the results are shown as fold-changes. (B) *Robo1*, *Robo2*, *Robo3* and *Robo4* expression was examined using real-time quantitative PCR and the data are expressed as described in A. All data are expressed as the mean ± SD (n=3).

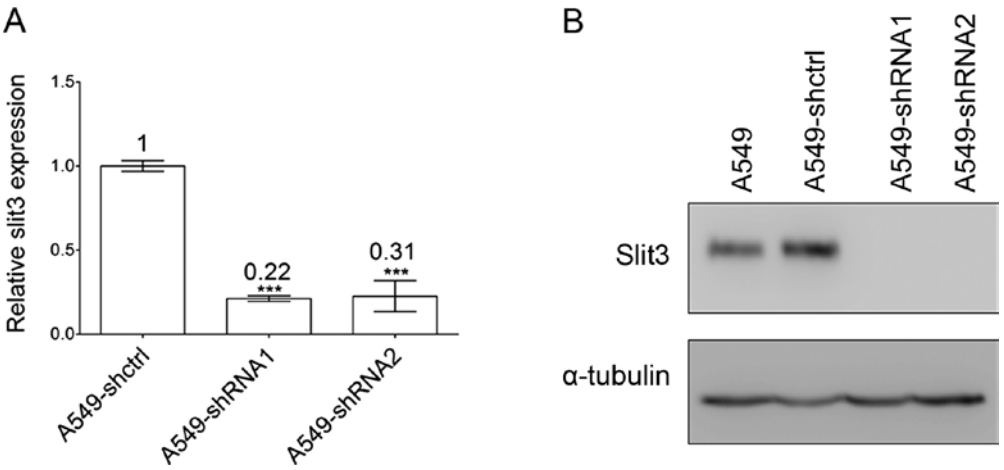

Figure 2. *Slit3* silencing in A549 cells. Cells were stably transduced with pLL3.7-*Slit3*-shRNA (A549-shRNA) or a control plasmid (A549-shctrl) as described in Materials and methods. Silencing of *Slit3* expression was analyzed by (A) real-time quantitative PCR. Data are expressed as the mean ± SD. Significant differences (***P<0.001, n=3) were determined by Student's t-test using GraphPad Prism 5.0 software. (B) Immunoblotting. Membrane-associated proteins in the A549 cells were isolated with the Qproteome Cell Compartment kit. A total of 180 and 50 μg of protein was loaded to detect Slit3 and α-tubulin, respectively.

(A549-shctrl). Silencing of *Slit3* mRNA in the A549 cells was first verified by real-time quantitative PCR. *Slit3* mRNA expression in the A549 cells was significantly decreased, with a knockdown efficiency of 78 and 69%, respectively (Fig. 2A). Given that Slit3 is predominantly membrane-associated, we isolated the membrane-associated proteins in the A549 cells using a Qproteome Cell Compartment kit to detect the changes in Slit3 protein levels. We did not detect Slit3 protein bands when using 60-120 μg of total loading protein, yet detected it when using 180 μg of total sample protein (Fig. 2B). The discordance between high *Slit3* mRNA expression and protein abundance suggests that post-translational mechanisms influenced Slit3 abundance in the A549 cells. The molecular size of the Slit3 protein band detected in the A549 cells was slightly larger than the theoretically calculated value of N-terminal Slit3 (~140 kDa), which reflects cellular glycosylation of the slit3 protein. The results are consistent with the findings that the majority of Slits are secreted in a membrane-associated manner. Notably, full-length Slit3 (~200 kDa) was not detected, indicating that proteolytically processed N-terminal Slit3 is the primary form of secreted Slit3 in the A549 cells.

Slit3 silencing induces EMT in A549 cells. *Slit3* silencing induced significant morphologic changes in the A549 cells as demonstrated by an elongated fibroblast-like morphology, a phenomenon reminiscent of EMT (Fig. 3). We further examined the effects of Slit3 on the expression of molecular hallmarks of EMT, including the epithelial marker E-cadherin and the mesenchymal marker vimentin. Immunoblotting analysis confirmed that E-cadherin protein expression was obviously reduced in the A549-shRNA cells when compared with the controls. Corresponding to reduced E-cadherin expression, vimentin expression was significantly increased.

Slit3 silencing enhances the proliferation, migration and invasion of A549 cells. To evaluate the effects of Slit3 on the proliferation of A549 cells with *Slit3* knockdown, the MTT assay was performed. Compared with the controls, the *Slit3*

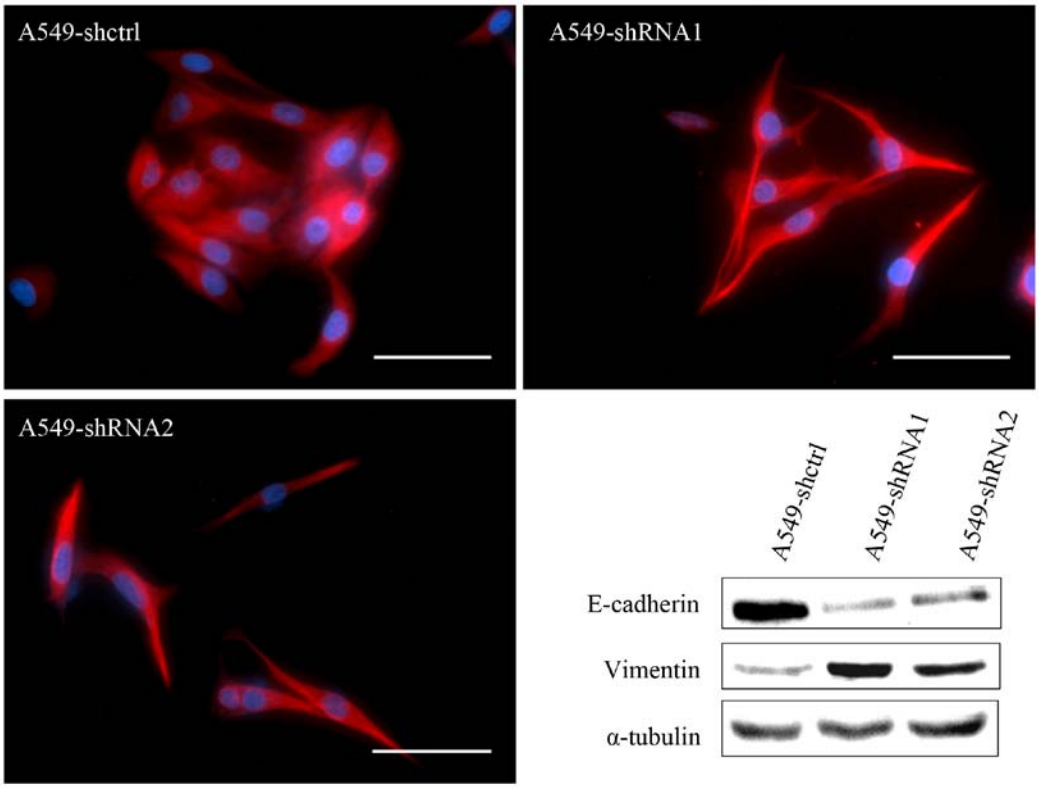

Figure 3. *Slit3* silencing induces EMT in A549 cells. Obvious morphologic changes were observed in the *Slit3*-knockdown A549 cells. Cells were cultured on 24-well microplates and stained for tubulin with Alexa Fluor 594 (red) and nuclear DNA with DAPI. Images were captured randomly under an inverted fluorescence microscope. Representative images are shown. Scale bar, 100 μm (magnification, x400). *Slit3* silencing in A549 cells led to reduced E-cadherin and increased vimentin expression (lower right).

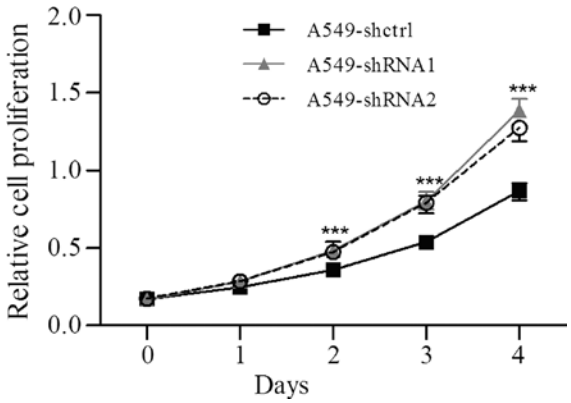

Figure 4. Effects of *Slit3* silencing on the proliferation of A549 cells. A549 cells were cultured in 96-well microplates for 4 consecutive days. MTT assays were performed each day (n=5). Results are shown as the mean ± SD. Significant differences (***P<0.001) were determined by Student's t-test using GraphPad Prism 5.0 software.

knockdown significantly stimulated the proliferation of the A549 cells (Fig. 4). Cell migration was measured by a wound healing assay in which the Slit3 knockdown significantly promoted the migration of the A549 cells when compared to that of the controls (Fig. 5A). Similar results were also observed in the Matrigel invasion assay. *Slit3* knockdown enhanced the ability of A549 cells to traverse the Matrigel-coated membrane (Fig. 5B). These results suggest that Slit3 exerts negative regulation on the proliferation and invasive behavior of A549 cells, thereby confirming the role of slit3 as a tumor suppressor.

Slit3 silencing upregulates MMP2 and MMP9 expression. To explore the mechanisms underlying the stimulative effects of Slit3 silencing on the invasion of A549 cells, we detected *MMP2* and *MMP9* expression, which are key enzymes for degradation of type IV collagen, a major component of the basement membrane. Quantitative PCR results showed that silencing of *Slit3* in the A549 cells caused significant upregulation of both *MMP2* and *MMP9* (Fig. 6A). To verify the effects of Slit3 silencing on MMP2 and MMP9 secretion, gelatin zymography was performed. Supernatants were prepared by incubating the cells with serum-free DMEM for 12 h to decrease the effects of cell proliferation on MMP production. As shown in Fig. 6B, A549 control cells maintained very weak MMP2 secretion, whereas MMP9 production was not detected. *Slit3* silencing in the A549 cells induced an increase in MMP2 production. Although MMP9 was not detected (Fig. 6B, left), *Slit3* silencing in the A549 cells caused significant upregulation of *MMP9* at the mRNA level (Fig. 6A). Lack of MMP9 detection could be due to low *MMP9* expression in A549 cells. Quantitative PCR confirmed that *MMP9* expression was significantly lower than *MMP2* in the A549 cells (data not shown). To determine whether weak *MMP2* and *MMP9* expression is common in lung carcinoma cell lines, culture supernatants from the Spc-a-1 and Ltep-a-2 cell lines were also assayed using gelatin

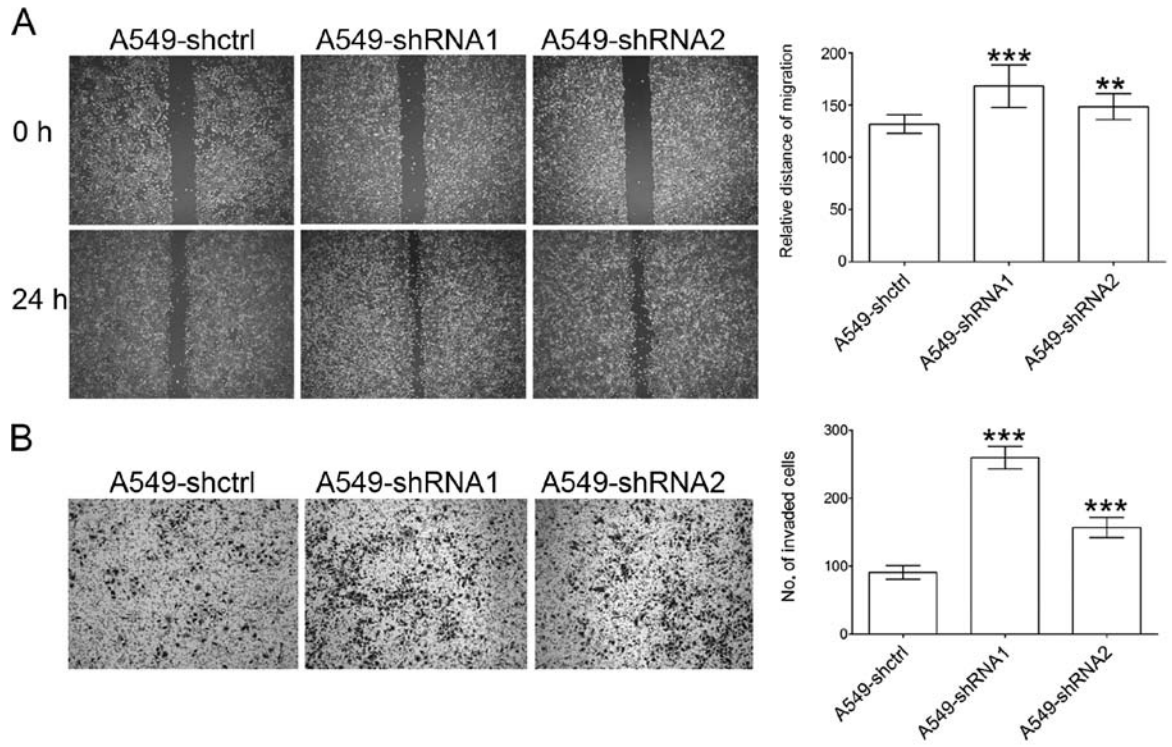

Figure 5. Effects of *Slit3* silencing on the migration and invasion of A549 cells. *Slit3* silencing in A549 cells promoted (A) migration (magnification x40, n=3) and (B) invasion (magnification x100, n=3). Results are shown as the mean ± SD. Significant differences ($^{**}P<0.01$, $^{***}P<0.001$) were determined by Student's t-test using GraphPad Prism 5.0 software.

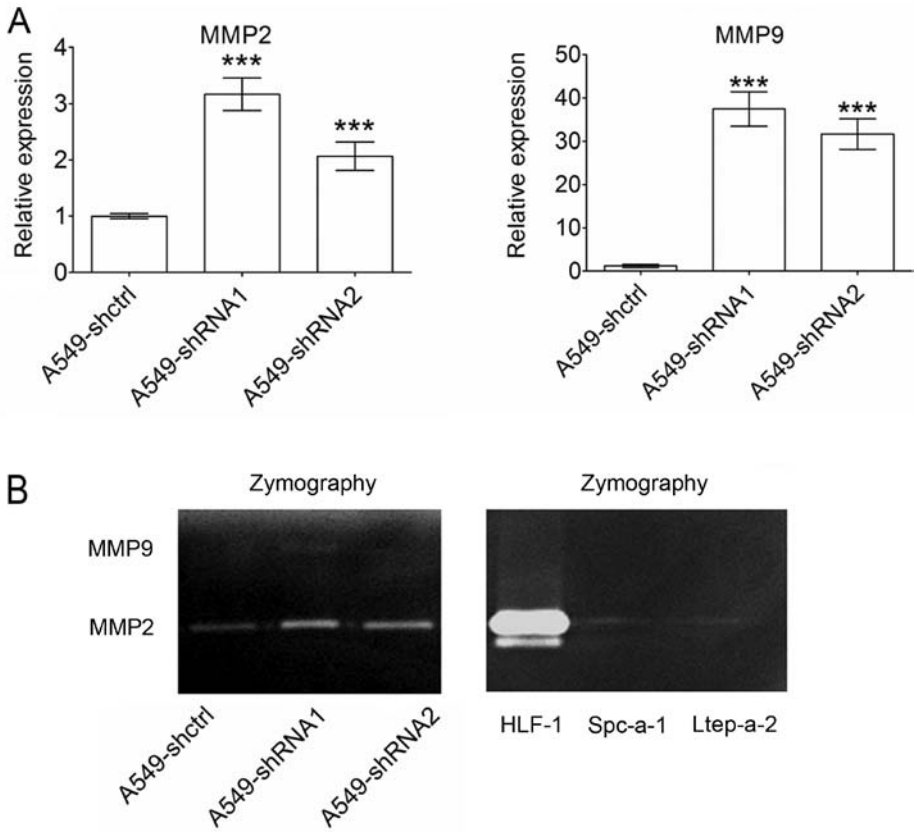

Figure 6. Effects of *Slit3* silencing on *MMP2* and *MMP9* expression in the A549 cells. (A) Real-time quantitative PCR. Each sample was analyzed in triplicate, and the results are expressed as fold-change. Data were first normalized to GAPDH and then normalized to the values of the control cells. Data are expressed as the mean ± SD. Significant differences ($^{***}P<0.001$, n=3) were determined by the Student's t-test using GraphPad Prism 5.0 software. (B) Zymography. Left: *Slit3* silencing in A549 cells increased MMP2 production, while no MMP9 production was detected. Right: Two lung carcinoma cell lines, Spc-a-1 and Ltep-a-2, showed weak MMP2 production. MMP9 was not detected, indicating that relatively weak *MMP2* and *MMP9* expression may be a common characteristic of lung carcinoma cell lines.

zymography. Human normal lung fibroblasts (HFL-1) were used as a positive control. HFL-1 maintained high levels of MMP2, while the two lung carcinoma cell lines showed weak MMP2 production. MMP9 was not detected in any of the cell lines (Fig. 6B, right). These results suggest that relatively weak *MMP2* and *MMP9* expression may be a common characteristic in the lung carcinoma cell lines analyzed.

Discussion

Although a number of studies have explored the roles of Slit2 in tumor progression, relatively little progress has been made in defining the effects of Slit3 on tumors. In contrast to *Slit2*, which was reported to be upregulated in various tumors (18,20), few results concerning *Slit3* upregulation in tumor tissues have been reported. Although microarray analysis revealed *Slit3* upregulation in separated invasive hepatocellular carcinoma cells, no evidence of protein level upregulation has been provided (37). Moreover, *Slit3* upregulation at the mRNA level does not necessarily lead to an increase in Slit3 at the protein level. Chen *et al* examined the correlation between mRNA expression and protein levels in lung adenocarcinomas and found a significant correlation in only a small subset of the proteins studied (38). Towner *et al* recently reported high *Slit3* expression on the surface of high-grade human gliomas compared to low-grade gliomas and normal brain tissues using immunohistochemistry and suggested Slit3 as a potent biomarker for human high-grade gliomas in clinical diagnosis (36). These results are in contrast to reports that *Slit3* is frequently methylated in gliomas (8), indicating heterogeneous *Slit3* expression in gliomas. The present study confirmed *Slit3* expression in the U87MG glioblastoma cell line and detected higher *Slit3* expression in lung carcinoma A549 cells. These results are consistent with reports that the frequency of promoter methylation is lower in lung carcinomas (8,29) and partially explained high *Slit3* expression in A549 cells. However, the high *slit3* expression in A549 cells was not confirmed in two other lung adenocarcinoma cell lines (Spc-a-1 and Ltep-a-2), indicating cell-specific *Slit3* expression that was not apparent at the protein level.

As in the U87MG cells, Slit3 proteins were not detected in the supernatant using ELISA. However, immunofluorescence detected a very weak signal on the cell surface, indicating that Slit3 in A549 cells remains mostly membrane-associated. Immunoblotting further validated the trace amounts of Slit3 associated with the cell membrane. These results suggest that post-translational mechanisms influence Slit3 protein abundance in cells despite mRNA expression. Given that Slit3 functions as a latent tumor suppressor, we suggest that post-translational regulation of *Slit3* confers a self-protective advantage against the tumor-suppressor effects of Slit3.

In contrast to the findings that both full length and N-terminal fragments of Slit are present in neuronal cells (39) or tissues (40), only the N-terminal of the Slit3 protein (~140 kDa) was detected at the A549 cell surface, indicating that the extent of proteolytic cleavage of the Slit3 protein differs by tissue type. The cleaved Slit fragment also exerts different functions. Nguyen *et al* demonstrated that full length Slit2 neutralized the branching of dorsal root ganglia axons induced by N-terminal Slit2 (41), suggesting that the function of Slit was partly associated with its structure. In the present study, lack of full length Slit3 in A549 cells may imply the loss of an unknown regulatory mechanism that balances the effects of the N-terminal Slit3 fragment.

Recombinant Slit3 was reported to inhibit the migration of malignant melanoma cells through downregulation of AP-1 (30). *Slit3* overexpression in human breast carcinoma cells inhibits tumor growth by suppressing *Sdf1* and *Cxcr4* expression (17). The present study indicated that *Slit3* silencing in A549 cells promoted proliferation, migration and invasion of the cells even though only trace amounts of Slit3 protein were detected. These results are evidence that Slit3 exerts negative regulatory effects on tumor proliferation and migration. Results are in accordance with reported suppressive effects of Slit2 on growth and migration in various types of tumor. In nervous system development, Slits function as repellent factors that prevent axon growth into particular regions (42). Increased migration due to Slit3 silencing supports the idea that repellent effects may also influence tumor cell migration.

EMT plays a critical role in tumor metastasis by which tumor cells weaken E-cadherin-dependent intercellular adhesion and enhance motility, facilitating tumor cells to invade surrounding tissues. Chen *et al* reported an inhibitory effect of Slit2 on EMT wherein *Slit2* overexpression in colorectal cancer cells inhibited cell migration as a result of increasing E-cadherin levels, while Slit2 knockdown led to opposite results (11). However, Slit2 promotion of EMT was also reported in colorectal cancer cells (21), the different cell lines analyzed accounted for conflicting results. The results of the present study confirmed the inhibitory effects of Slit3 on EMT in lung carcinoma A549 cells given that Slit3 silencing induced an elongated fibroblast-like morphology, downregulation of E-cadherin and upregulation of vimentin.

MMPs play a critical role in tumor metastasis. The prometastatic or antimetastatic effects of Slit are likely associated with MMP expression or protein activities. Qi *et al* recently reported upregulation of MMP2, yet not MMP9 in skin tissue of Slit2-transgenic mice and proposed that MMP2 upregulation accounted for loss of the basement membrane in Slit2-transgenic mice, indicating a positive correlation between Slit2 and MMP2 expression (20). However, Prasad *et al* reported that Slit2 inhibits the CXCL12-induced activities of MMP2 and MMP9 in breast cancer cells (43). Our results showed that MMP2 and MMP9 expression was negatively associated with alteration of *Slit3* expression. *Slit3* silencing promoted MMP2 and MMP9 expression in A549 cells, whereas *Slit3* overexpression reduced expression, supporting the negative correlation between Slit3 and MMP2 and MMP9 expression, even though only MMP2 secretion was detected. Conflicting results, however, were recently reported in primary amnion and myometrial cells wherein *Slit3* knockdown with siRNA decreased MMP9 gene expression and secretion (44). Mechanisms underlying these results may be associated with heterogeneous expression of Robo receptors in various tissues. Of the four Robo receptors, Robo4 is structurally divergent from the other three members both in extracellular and intracellular domains and may stimulate signaling pathways that differ from other receptors, resulting in a functional difference. For example, Slit2/Robo4 and Slit2/Robo1 signaling pathways induce opposite effects on the migration of endothelial cells (45). In the present study, Robo1 and Robo4 were detected

in A549 cells and Robo1 maintained a relatively high level of expression. Therefore, we suggest that Slit3 most likely exerts its effects in A549 cells by binding to Robo1.

In summary, these results demonstrated that Slit3 functions as a tumor suppressor in lung carcinoma. Due to promoter hypermethylation, overall expression of *Slit3* is downregulated in most tumors. Even if hypomethylation of the promoter occurs in some cancer tissues, such as lung carcinoma, and results in high slit3 expression, transcription of the slit3 protein is still strictly controlled. Slit3 represses migration and invasion of A549 cells by blocking EMT and suppressing both MMP2 and MMP9 expression and secretion. Further studies are needed to decipher the mechanisms underlying the post-translational regulation of Slit3 and suppression of MMP2 and MMP9 expression and secretion.

Acknowledgements

This study was supported by grants of National Natural Science Foundation of China (grant no. 30971210), the Key Project of Chinese Ministry of Education (grant no. 109093) and the Fujian Provincial Department of Science and Technology (grant no. 2007J0113).

References

1. Katoh Y and Katoh M: Comparative genomics on *SLIT1*, *SLIT2*, and *SLIT3* orthologs. Oncol Rep 14: 1351-1355, 2005.
2. Brose K, Bland KS, Wang KH, Arnott D, Henzel W, Goodman CS, Tessier-Lavigne M and Kidd T: Slit proteins bind Robo receptors and have an evolutionarily conserved role in repulsive axon guidance. Cell 96: 795-806, 1999.
3. Patel K, Nash JA, Itoh A, Liu Z, Sundaresan V and Pini A: Slit proteins are not dominant chemorepellents for olfactory tract and spinal motor axons. Development 128: 5031-5037, 2001.
4. Condac E, Strachan H, Gutierrez-Sanchez G, Brainard B, Giese C, Heiss C, Johnson D, Azadi P, Bergmann C, Orlando R, *et al*: The C-terminal fragment of axon guidance molecule Slit3 binds heparin and neutralizes heparin's anticoagulant activity. Glycobiology 22: 1183-1192, 2012.
5. Wu JY, Feng L, Park HT, Havlioglu N, Wen L, Tang H, Bacon KB, Jiang Zh, Zhang Xc and Rao Y: The neuronal repellent Slit inhibits leukocyte chemotaxis induced by chemotactic factors. Nature 410: 948-952, 2001.
6. Shyamsundar R, Kim YH, Higgins JP, Montgomery K, Jorden M, Sethuraman A, van de Rijn M, Botstein D, Brown PO and Pollack JR: A DNA microarray survey of gene expression in normal human tissues. Genome Biol 6: R22, 2005.
7. Dallol A, Da Silva NF, Viacava P, Minna JD, Bieche I, Maher ER and Latif F: *SLIT2*, a human homologue of the *Drosophila Slit2* gene, has tumor suppressor activity and is frequently inactivated in lung and breast cancers. Cancer Res 62: 5874-5880, 2002.
8. Dickinson RE, Dallol A, Bieche I, Krex D, Morton D, Maher ER and Latif F: Epigenetic inactivation of *SLIT3* and *SLIT1* genes in human cancers. Br J Cancer 91: 2071-2078, 2004.
9. Dallol A, Krex D, Hesson L, Eng C, Maher ER and Latif F: Frequent epigenetic inactivation of the *SLIT2* gene in gliomas. Oncogene 22: 4611-4616, 2003.
10. Dunwell TL, Dickinson RE, Stankovic T, Dallol A, Weston V, Austen B, Catchpoole D, Maher ER and Latif F: Frequent epigenetic inactivation of the *SLIT2* gene in chronic and acute lymphocytic leukemia. Epigenetics 4: 265-269, 2009.
11. Chen WF, Gao WD, Li QL, Zhou PH, Xu MD and Yao LQ: SLIT2 inhibits cell migration in colorectal cancer through the AKT-GSK3β signaling pathway. Int J Colorectal Dis 28: 933-940, 2013.
12. Kim HK, Zhang H, Li H, Wu TT, Swisher S, He D, Wu L, Xu J, Elmets CA, Athar M, *et al*: Slit2 inhibits growth and metastasis of fibrosarcoma and squamous cell carcinoma. Neoplasia 10: 1411-1420, 2008.
13. Göhrig A, Detjen KM, Hilfenhaus G, Körner JL, Welzel M, Arsenic R, Schmuck R, Bahra M, Wu JY, Wiedenmann B, *et al*: Axon guidance factor SLIT2 inhibits neural invasion and metastasis in pancreatic cancer. Cancer Res 74: 1529-1540, 2014.
14. Werbowetski-Ogilvie TE, Seyed Sadr M, Jabado N, Angers-Loustau A, Agar NY, Wu J, Bjerkvig R, Antel JP, Faury D, Rao Y, *et al*: Inhibition of medulloblastoma cell invasion by Slit. Oncogene 25: 5103-5112, 2006.
15. Dallol A, Morton D, Maher ER and Latif F: *SLIT2* axon guidance molecule is frequently inactivated in colorectal cancer and suppresses growth of colorectal carcinoma cells. Cancer Res 63: 1054-1058, 2003.
16. Qiu H, Zhu J, Yu J, Pu H and Dong R: SLIT2 is epigenetically silenced in ovarian cancers and suppresses growth when activated. Asian Pac J Cancer Prev 12: 791-795, 2011.
17. Marlow R, Strickland P, Lee JS, Wu X, Pebenito M, Binnewies M, Le EK, Moran A, Macias H, Cardiff RD, *et al*: SLITs suppress tumor growth in vivo by silencing *Sdf1/Cxcr4* within breast epithelium. Cancer Res 68: 7819-7827, 2008.
18. Wang B, Xiao Y, Ding BB, Zhang N, Yuan X, Gui L, Qian KX, Duan S, Chen Z, Rao Y, *et al*: Induction of tumor angiogenesis by Slit-Robo signaling and inhibition of cancer growth by blocking Robo activity. Cancer Cell 4: 19-29, 2003.
19. Wang LJ, Zhao Y, Han B, Ma YG, Zhang J, Yang DM, Mao JW, Tang FT, Li WD, Yang Y, *et al*: Targeting Slit-Roundabout signaling inhibits tumor angiogenesis in chemical-induced squamous cell carcinogenesis. Cancer Sci 99: 510-517, 2008.
20. Qi C, Lan H, Ye J, Li W, Wei P, Yang Y, Guo S, Lan T, Li J, Zhang Q, *et al*: Slit2 promotes tumor growth and invasion in chemically induced skin carcinogenesis. Lab Invest 94: 766-776, 2014.
21. Zhou WJ, Geng ZH, Chi S, Zhang W, Niu XF, Lan SJ, Ma L, Yang X, Wang LJ, Ding YQ, *et al*: Slit-Robo signaling induces malignant transformation through Hakai-mediated E-cadherin degradation during colorectal epithelial cell carcinogenesis. Cell Res 21: 609-626, 2011.
22. Yang XM, Han HX, Sui F, Dai YM, Chen M and Geng JG: Slit-Robo signaling mediates lymphangiogenesis and promotes tumor lymphatic metastasis. Biochem Biophys Res Commun 396: 571-577, 2010.
23. Liu J, Zhang L, Wang D, Shen H, Jiang M, Mei P, Hayden PS, Sedor JR and Hu H: Congenital diaphragmatic hernia, kidney agenesis and cardiac defects associated with Slit3-deficiency in mice. Mech Dev 120: 1059-1070, 2003.
24. Yuan W, Rao Y, Babiuk RP, Greer JJ, Wu JY and Ornitz DM: A genetic model for a central (septum transversum) congenital diaphragmatic hernia in mice lacking *Slit3*. Proc Natl Acad Sci USA 100: 5217-5222, 2003.
25. Zhang B, Dietrich UM, Geng JG, Bicknell R, Esko JD and Wang L: Repulsive axon guidance molecule Slit3 is a novel angiogenic factor. Blood 114: 4300-4309, 2009.
26. Paul JD, Coulombe KL, Toth PT, Zhang Y, Marsboom G, Bindokas VP, Smith DW, Murry CE and Rehman J: SLIT3-ROBO4 activation promotes vascular network formation in human engineered tissue and angiogenesis in vivo. J Mol Cell Cardiol 64: 124-131, 2013.
27. Narayan G, Goparaju C, Arias-Pulido H, Kaufmann AM, Schneider A, Dürst M, Mansukhani M, Pothuri B and Murty VV: Promoter hypermethylation-mediated inactivation of multiple Slit-Robo pathway genes in cervical cancer progression. Mol Cancer 5: 16, 2006.
28. Nones K, Waddell N, Song S, Patch AM, Miller D, Johns A, Wu J, Kassahn KS, Wood D, Bailey P, *et al*: Genome-wide DNA methylation patterns in pancreatic ductal adenocarcinoma reveal epigenetic deregulation of SLIT-ROBO, ITGA2 and MET signaling. Int J Cancer 135: 1110-1118, 2014.
29. Dammann R, Strunnikova M, Schagdarsurengin U, Rastetter M, Papritz M, Hattenhorst UE, Hofmann HS, Silber RE, Burdach S and Hansen G: CpG island methylation and expression of tumour-associated genes in lung carcinoma. Eur J Cancer 41: 1223-1236, 2005.
30. Denk AE, Braig S, Schubert T and Bosserhoff AK: Slit3 inhibits activator protein 1-mediated migration of malignant melanoma cells. Int J Mol Med 28: 721-726, 2011.
31. Schubert T, Denk AE, Ruedel A, Kaufmann S, Hustert E, Bastone P and Bosserhoff AK: Fragments of SLIT3 inhibit cellular migration. Int J Mol Med 30: 1133-1137, 2012.
32. Guan H, Wei G, Wu J, Fang D, Liao Z, Xiao H, Li M and Li Y: Down-regulation of miR-218-2 and its host gene SLIT3 cooperate to promote invasion and progression of thyroid cancer. J Clin Endocrinol Metab 98: E1334-E1344, 2013.

33. Livak KJ and Schmittgen TD: Analysis of relative gene expression data using real-time quantitative PCR and the $2^{-\Delta\Delta C_T}$ method. Methods 25: 402-408, 2001.
34. Bhattacharjee A, Richards WG, Staunton J, Li C, Monti S, Vasa P, Ladd C, Beheshti J, Bueno R, Gillette M, *et al*: Classification of human lung carcinomas by mRNA expression profiling reveals distinct adenocarcinoma subclasses. Proc Natl Acad Sci USA 98: 13790-13795, 2001.
35. Hou J, Aerts J, den Hamer B, van Ijcken W, den Bakker M, Riegman P, van der Leest C, van der Spek P, Foekens JA, Hoogsteden HC, *et al*: Gene expression-based classification of non-small cell lung carcinomas and survival prediction. PLoS One 5: e10312, 2010.
36. Towner RA, Jensen RL, Vaillant B, Colman H, Saunders D, Giles CB and Wren JD: Experimental validation of 5 in-silico predicted glioma biomarkers. Neuro Oncol 15: 1625-1634, 2013.
37. Lin ZY and Chuang WL: Genes responsible for the characteristics of primary cultured invasive phenotype hepatocellular carcinoma cells. Biomed Pharmacother 66: 454-458, 2012.
38. Chen G, Gharib TG, Huang CC, Taylor JM, Misek DE, Kardia SL, Giordano TJ, Iannettoni MD, Orringer MB, Hanash SM, *et al*: Discordant protein and mRNA expression in lung adenocarcinomas. Mol Cell Proteomics 1: 304-313, 2002.
39. Hu H: Chemorepulsion of neuronal migration by Slit2 in the developing mammalian forebrain. Neuron 23: 703-711, 1999.
40. Niclou SP, Jia L and Raper JA: Slit2 is a repellent for retinal ganglion cell axons. J Neurosci 20: 4962-4974, 2000.
41. Nguyen Ba-Charvet KT, Brose K, Ma L, Wang KH, Marillat V, Sotelo C, Tessier-Lavigne M and Chédotal A: Diversity and specificity of actions of Slit2 proteolytic fragments in axon guidance. J Neurosci 21: 4281-4289, 2001.
42. Bagri A, Marín O, Plump AS, Mak J, Pleasure SJ, Rubenstein JL and Tessier-Lavigne M: Slit proteins prevent midline crossing and determine the dorsoventral position of major axonal pathways in the mammalian forebrain. Neuron 33: 233-248, 2002.
43. Prasad A, Fernandis AZ, Rao Y and Ganju RK: Slit protein-mediated inhibition of CXCR4-induced chemotactic and chemoinvasive signaling pathways in breast cancer cells. J Biol Chem 279: 9115-9124, 2004.
44. Lim R, Barker G and Lappas M: SLIT3 is increased in supracervical human foetal membranes and in labouring myometrium and regulates pro-inflammatory mediators. Am J Reprod Immunol 71: 297-311, 2014.
45. Autiero M, De Smet F, Claes F and Carmeliet P: Role of neural guidance signals in blood vessel navigation. Cardiovasc Res 65: 629-638, 2005.